Am J Transl Res 2018;10(4):1143-1154
www.ajtr.org /ISSN:1943-8141/AJTR0073869

Original Article

Interleukin-6 from subchondral bone mesenchymal stem cells contributes to the pathological phenotypes of experimental osteoarthritis

Xiaofeng Wu[1,2], Lei Cao[2], Fan Li[2], Chao Ma[3], Guangwang Liu[3], Qiugen Wang[1,2]

[1]Nanjing Medical University, Nanjing 211166, China; [2]Department of Trauma Orthopaedic, Shanghai General Hospital of Nanjing Medical University, Shanghai 200080, China; [3]Department of Orthopedic Surgery, Xuzhou Central Hospital, Xuzhou Clinical School of Xuzhou Medical University, The Affiliated Xuzhou Hospital of Medical College of Southeast University, Xuzhou Clinical Medical College of Nanjing University of Chinese Medicine, Xuzhou 221009, Jiangsu, China

Received February 1, 2018; Accepted February 23, 2018; Epub April 15, 2018; Published April 30, 2018

Abstract: As a main cause of morbidity in the aged population, osteoarthritis (OA) is characterized by cartilage destruction, synovium inflammation, osteophytes, and subchondral bone sclerosis. To date its etiology remains elusive. Recent data highlight an important role of subchondral bone in the onset and progression of OA. Therefore, elucidating the mechanisms underlying abnormal subchondral bone could be of importance in the treatment of OA. Interleukin-6 is a proinflammatory cytokine involved in many physiological and pathological processes. Although *in vitro* and *in vivo* studies have indicated that IL-6 is an important cytokine in the physiopathogenesis of OA, its effects on subchondral bone have not been studied in OA animal models. In this study, we aimed to i) investigate the role of IL-6 in the pathological phenotypes of OA subchondral bone MSCs including increase in cell numbers, mineralization disorder and abnormal type I collagen production; ii) explore whether the systemic blockade of IL-6 signaling could alleviate the pathological phenotypes of experimental OA. We found that IL-6 was over-secreted by OA subchondral bone MSCs compared with normal MSCs and IL-6/STAT3 signaling was over-activated in subchondral bone MSCs, which contributed to the pathological phenotypes of OA subchondral bone MSCs. More importantly, systemic inhibition of IL-6/STAT3 signaling with IL-6 antibody or STAT3 inhibitor AG490 decreased the severity of pathological phenotypes of OA subchondral bone MSCs and cartilage lesions in OA. Our findings provide strong evidence for a pivotal role for IL-6 signaling in OA and open up new therapeutic perspectives.

Keywords: Osteoarthritis, Interleukin-6, mesenchymal stem cells, subchondral bone, STAT3

Introduction

As a main cause of morbidity in the aged population, osteoarthritis (OA) is characterized by cartilage destruction, synovium inflammation, osteophytes, and subchondral bone sclerosis. To date its etiology remains an open question. Recent data highlight an important role of subchondral bone in the onset and/or progression of OA [1-3]. Therefore, elucidating the mechanisms underlying bone sclerosis could be of importance in the treatment of OA, since bone sclerosis in OA increases mechanical stress to the overlying cartilage [4]. Bone sclerosis could lead to enhanced bone mineral density (BMD) in OA patients. However, enhanced BMD does not mean increased bone tissue density [5, 6] and does not mean better mechanical properties of OA bone tissue [7, 8]. Moreover, microCT analysis of human OA bone tissue revealed abnormal microstructure and organization of this tissue [8].

Interleukin 6 (IL-6) blockade has been shown to be effective in various musculoskeletal disorders, in particular rheumatoid arthritis (RA) [9]. Although *in vitro* and *in vivo* studies have indicated that IL-6 is an important cytokine in the physiopathogenesis of OA, the effect of systemic IL-6 inhibition on abnormal subchondral bone, an essential feature of OA, has not been studied in OA animal models, nor in humans.

IL-6 is a pleiotropic proinflammatory cytokine involved in many physiological and pathological processes [10]. It belongs to a family of gp130

cytokines. IL-6 binds firstly to its non-signaling specific receptor (IL-6R) and then to a common subunit gp130, which activates two main signaling pathways: signal transducer and activator of transcription (STAT) and extracellular signal-regulated kinase (ERK) [11]. Stat1, 3 and 5 are all activated by IL-6, but Stat3 is the main signaling factor downstream of IL-6 [12].

There is a close relationship between IL-6 serum levels and two major risk factors of knee OA: obesity and metabolic syndrome [13]. Data from a prospective cohort study indicated that higher serum level of IL-6 and body mass index (BMI) were independent predictors of incident radiographic knee OA [14]. High level of IL-6 are not only observed in knee OA synovial fluid and surrounding tissues at the onset of OA [15, 16], but is involved in the progression of knee OA after meniscectomy [17]. Within the joint, several tissues including synoviocytes, chondrocytes and subchondral bone mesenchymal stem cells (MSCs) can secret IL-6 in response to different stimulations, such as mechanical loading [18, 19]. The infrapatellar fat pad from knee OA patients can stimulate the secretion of IL-6 by synoviocytes [20]. In bovine chondrocytes, IL-6 increases the mRNA expression levels of matrix metalloproteinase 1 (Mmp1), 3 and 13, and a disintegrin and metalloproteinase with thrombospondin motifs 4 (Adamts4) and 5 [21]. Intra-articular injections of IL-6 reproduced OA-like cartilage destruction in mice, and IL-6 knockout (KO) mice develop less severe posttraumatic OA lesions [22].

In this study, we aimed to i) investigate the role of IL-6 in the pathological phenotypes of OA subchondral bone MSCs including increase in cell numbers, mineralization disorder and abnormal type I collagen production; ii) explore whether the systemic blockade of IL-6 signaling could alleviate the pathological phenotypes of experimental OA mouse. We found that IL-6 was over-secreted by OA subchondral bone MSCs compared with normal MSCs and IL-6/STAT3 signaling was over-activated in subchondral bone MSCs, which contributed to the pathological phenotypes of OA subchondral bone MSCs. More importantly, systemic inhibition of IL-6/STAT3 signaling with IL-6 antibody or STAT3 inhibitor AG490 decreased the severity of pathological phenotypes of OA subchondral bone MSCs and cartilage lesions in OA. Our findings provide strong evidence for a pivotal role for IL-6 signaling in OA and open up new therapeutic perspectives.

Materials and methods

Animals and OA mouse model

Anterior cruciate ligament transaction (ACLT) was performed in 8-week-old male C57BL/6 mice to induce OA as described [23]. Sham controls were done on independent mice. In a first assay, mice received intraperitoneal injections of an IL-6 antibody (#BE0046, BioXcell, 0.5 mg once a week) (n=10) or an IgG isotype control (#BE0088, BioXcell) (n=10) for 8 weeks from the day after the ACLT. In a second assay, the mice were treated daily with an intraperitoneal injection of AG490 (0.5 mg every other day, n=10) or DMSO vehicle control (n=10) for 8 weeks from the day after the ACLT. At week 8 after ACLT, knee joint samples were harvested from osteoarthritic mouse and sham controls.

Histology

Knee joint samples were fixed in 4% paraformadehyde, decalcified in 20% formic acid, and embedded with paraffin. 5 μm-thick serial sections were cut through the medial knee joints. Hematoxylin & orange G (H&OG) stained sections were scored according to the OARSI recommended 0-6 subjective scoring system [24]. In addition, cartilage proteoglycan loss was scored (on a scale of 0-3) for the complement of cartilage destruction [25]. The cartilage destruction severity was expressed as a summed score (sum of the 5 highest scores) and as a maximal score for the medial femora and tibiae separately within each joint.

MSCs isolation, in vitro culture and osteogenesis

The bone marrow from tibia subchondral bone were suspended in cold PBS with 2% FBS and passed through a 70 μm filter. Filtered bone marrow cells were suspended in PBS with 2% FBS and 0.1 g/L phenol red and then enriched for lineage negative (Lin-) cells using the SpinSep system (Stem Cell Technologies, Vancouver, BC, Canada). The cells were incubated with a murine progenitor enrichment cocktail (Stem Cell Technologies) on ice for 30 min, washed, and then incubated with dense particles on ice for 20 min. The cells were then centrifuged at

1200 g for 10 min, and the cells at the density medium/PBS interface were collected.

Enriched MSCs were seeded onto culture plates at a density of 0.1×10^6 cells/cm^2 in alpha-MEM containing 100 units/ml penicillin (Gibco) and 100 μg/ml streptomycin (Gibco). The media were changed after 72 h and adherent cells were maintained in culture with twice weekly media changes.

To induce osteogenic differentiation, MSCs were treated with 100 nM dexamethasone, 10 mM β-glycerophosphate disodium and 50 μg/ml ascorbic acid.

Alizarin red staining and quantification

Osteoblast maturation was evaluated by mineralized nodules stained with Alizarin Red. After fixation, the cells were washed with cold PBS and incubated in 40 mM Alizarin Red (pH 4.2) for 30 min at 37°C, then washed with PBS and imaged.

Decalcification was performed using 0.1 M HCl overnight at 4°C. Then, 20 μL of samples were transferred to the test tubes containing 1 mL of methyl thymol blue solution and 1 mL of alkaline solution. Absorbance was determined at 610 nm.

Immunohistochemistry

Immunohistochemistry was performed according to standard protocol. Sections were incubated with primary antibodies against mouse nestin (Invitrogen Antibodies), osterix (Abcam), IL-6 (Abcam) and p-STAT3 (Tyr705, Cell signaling technology) overnight at 4°C. For immunohistochemical staining, a horse radish peroxidas-streptavidin detection system (Dako) was used to detect the immunoactivity followed by counterstaining with hematoxylin (Dako).

Flow cytometry

Mice were sacrificed and tibia subchondral bone marrow cells were harvested and pooled together. After red blood cells were lysed, the bone marrow cells were centrifuged and then the cell pellet was resuspended and fixed in 4% paraformaldehyde. Cells were permeabilized in 0.1% Triton X-100 and then blocked in blocking buffer (PBS with 3% FBS and 0.1% sodium azide) for 30 min on ice. Then the cells were incubated with anti-nestin antibody (Invitrogen Antibodies), anti-osterix antibody (Abcam) or isotype control for 1 h at 37°C in dark room, and then washed twice with PBS with 0.1% BSA. The cells were incubated with fluorochrome-conjugatd secondary antibody for 30 min on ice. Probes were analyzed using a BD Calibur flow cytometer and CellQuest software (Becton Dickinson).

qRT-PCR

Total RNA was isolated using an RNeasy Mini Kit (Qiagen, Valencia, CA, USA). cDNA was synthesized from 1 μg of total RNA. Quantitative PCR was performed using the ABI Prism 7500 (Applied BioSystems, Foster City, CA, USA) and the SYBR Green PCR Master Mix (Takara Bio Inc., Otsu, Japan). The cycling conditions were as follows: 94°C for 30 s followed by 40 cycles of 94°C for 5 s and 60°C for 34 s. The $2^{-\Delta\Delta Ct}$ method was used to calculate the relative expression of each target gene. GAPDH was used as an internal control. The primer sequences are listed as follows: IL-6: 5'-GCCTTCTTGGGACTGATGCT-3' (forward), 5'-TGCCATTGCACAACTCTTTTCT-3' (reverse); Col1A1: 5'-GAGAGGTGAACAAGGTCCCG-3' (forward), 5'-AAACCTCTCTCGCCTCTTGC-3' (reverse); Col1A2: 5'-CCCAGAGTGGAACAGCGATT-3' (forward), 5'-ATGAGTTCTTCGCTGGGGTG-3' (reverse); GAPDH: 5'-CCCTTAAGAGGGATGCTGCC-3' (forward), 5'-TACGGCCAAATCCGTTCACA-3' (reverse).

Western blot

Cells were lysed on ice for 30 min in a lysis buffer (50 mM Tris-HCl, 150 mM NaCl, 1% Nonidet P-40, and 0.1% SDS supplemented with protease inhibitors). The proteins were separated by SDS-PAGE, transferred to a PVDF membrane, and detected using anti-IL-6 (Cell Signaling Technology, Danvers, MA, USA), anti-p-STAT3 (Y705) (Cell Signaling Technology), anti-STAT3 (Cell Signaling Technology), anti-Col1A1 (Abcam), anti-Col1A2 (Invitrogen Antibodies) and anti-GAPDH (Cell Signaling Technology) antibodies. The proteins were visualized using an enhanced chemiluminescence system (GE Healthcare, Piscataway, NJ, USA).

In vitro neutralization of IL-6

To block the IL-6 activity *in vitro*, IL-6 neutralization antibody (Peprotech, Rocky Hill, NJ, USA)

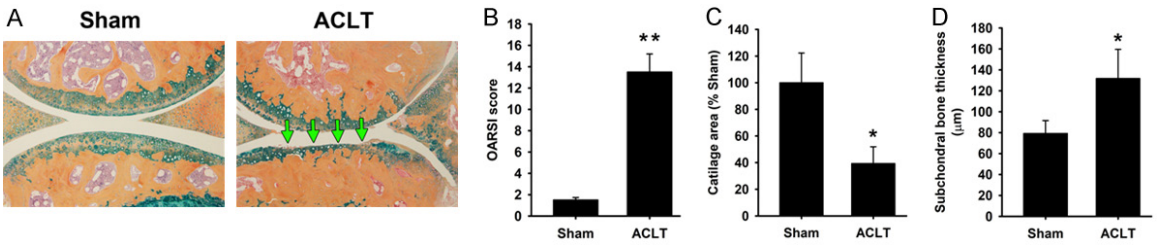

Figure 1. Cartilage degradation and subchondral bone sclerosis in ACLT osteoarthritis (OA) mouse. Anterior cruciate ligament transaction (ACLT) was performed in 8-week-old male C57BL/6 mice to induce OA. 8 weeks after surgery, histological changes in knee joints were analyzed between OA mice and sham controls by AB/H&OG staining (A). Green arrows indicated cartilage destructions. The summed OARSI scores of articular cartilage histologic structure were compared in OA mice or sham controls (B). The cartilage area of tibia was quantified through Bioquant software in OA mice and sham controls (C). The subchondral bone thickness of tibia was quantified in OA mice and sham controls (D). Data are shown as the means ± SD. *: P<0.05, **: P<0.01, ACLT *vs.* Sham.

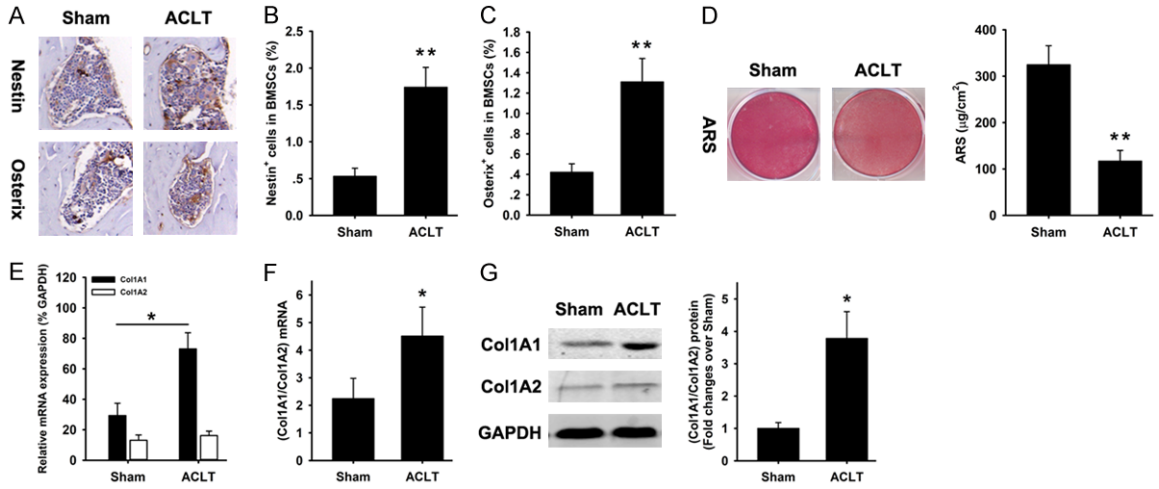

Figure 2. Increase in cell numbers, mineralization disorder and abnormal type I collagen production of subchondral bone MSCs in ACLT OA mouse. Immunostainings for nestin and osterix were employed to analyze the number of MSCs in the subchondral bone marrow of OA mice compared to sham controls (A). Flow cytometry was performed to confirm the results from immunostainings (B and C). MSCs were harvested from subchondral bone of OA mice and sham controls, cultured *in vitro* and induced to undergo osteogenic differentiation. Alizarin red staining was employed to evaluate the mineralization ability of these MSCs (D). Quantitative RT-PCR was performed to investigate the mRNA expression levels of col1A1 and col1A2 in OA MSCs compared with normal MSCs (E) and the ratio of col1A1 to col1A2 mRNA was calculated (F). GAPDH was used as an internal control. The results are expressed as the percentage of GAPDH. Western blot using col1A1 and col1A2 antibodies was performed to confirm the results from qRT-PCR (G). GAPDH was used as an internal control. Protein bands density was measured using image software. The relative protein expression level was normalized to GAPDH. Data are shown as the means ± SD. *: P<0.05, **: P<0.01, ACLT *vs.* Sham.

was added to the cell culture medium at a concentration of 0.8 μg/ml. IgG was used as control.

RNAi

Plasmid vector loading shRNAs against IL-6 for lentivirus packaging were purchased from Genecopoeia (Rockville, MD, USA). 293T cells were plated and the transfection complex was added to the culture medium at 293T 70-80% confluence. Then the cells were incubated in a CO_2 incubator at 37°C for 48 h and the medium was then collected. Lentivirus titer was evaluated by Lenti-X p24 Rapid titer kit (Clontech, Mountain View, CA, USA). After infection of MSCs by lentivirus loading shRNAs against IL-6, RT-PCR was perormed to analyze IL-6 expression.

Statistical analysis

Statistical significance was calculated by Student's t-test for two-sample comparisons using

the software SPSS 16.0. Statistical significance was determined using data from at least three independent experiments. $P<0.05$ were defined as significant. All of the data are presented as the mean ± SD unless otherwise specified.

Results

Cartilage degradation and subchondral bone sclerosis in ACLT OA mouse

ACLT was performed in C57BL/6 mice to generate a destabilized OA model. 8 weeks after surgery, histological changes in knee joints were analyzed between OA mice and sham controls. Sham knee joints were normal, indicated by AB/H&OG staining (**Figure 1A**). In contrast, remarkable cartilage degenerations and proteoglycans loss were observed in the OA knee joints (**Figure 1A**). To quantify the severity of cartilage damage, we compared the scores of articular cartilage histologic structure between OA mice and sham controls. The summed OARSI scores for morphological structure changes were significantly greater in the knee joints of OA mice than sham controls (**Figure 1B**). Also, the cartilage area of tibia was quantified through Bioquant software. A 60% decrease in the tibia cartilage area was observed in OA mice compared with sham controls (**Figure 1C**).

To analyze the changes of subchondral bone in OA knee joints, the subchondral bone thickness of tibia was quantified. A 60% increase in the subchondral bone thickness of tibia was observed in OA mice compared with sham controls (**Figure 1D**), suggesting that there was sclerosis in subchondral bone area of OA mice.

Increase in cell numbers, mineralization disorder and abnormal type I collagen production of subchondral bone MSCs in ACLT OA mouse

In the current study, we focused on the abnormal changes of subchondral bone in OA mice. Bone formation is resulted from osteogenic differentiation of bone marrow MSCs. Therefore, following the analysis of the pathological phenotypes of articular cartilage and subchondral bone in osteoarthritis, the changes of MSCs in subchondral bone were then investigated. Immunostaining for nestin, primarily expressed in adult bone marrow MSCs [23], revealed a significantly higher number of nestin$^+$ cells in the subchondral bone of OA mice compared to sham controls (**Figure 2A**). Once committed to the osteoblast lineage, MSCs express osterix, a marker of osteoprogenitors. The number of osterix$^+$ osteoprogenitors also significantly increased in the subchondral bone of OA mice compared to sham controls (**Figure 2A**), indicating nestin$^+$ MSCs undergo osteoblastic differentiation for *de novo* bone formation. These results were confirmed in flow cytometry analysis. A 2-fold increase in the number of nestin$^+$ MSCs (**Figure 2B**) and osterix$^+$ osteoprogenitors (**Figure 2C**) from subchondral bone was observed in OA mice compared with sham controls.

Having observed the increased number of MSCs from subchondral bone in OA, we then evaluated the functions of these cells. MSCs were harvested from subchondral bone, cultured *in vitro* and induced to undergo osteogenic differentiation. Alizarin red staining was employed to evaluate the mineralization ability of these MSCs. The significant attenuation of staining was observed in OA subchondral bone MSCs compared with sham controls (**Figure 2D**). These results were supported by the Alizarin red quantification (**Figure 2D**), suggesting that the mineralization ability of OA subchondral bone MSCs was weaker than normal MSCs although their number was more than normal MSCs.

Blunted mineralization could be attributed to abnormal production of type I collagen in OA MSCs [26]. As shown in **Figure 2E**, a 2.4-fold higher expression of col1A1 mRNA was observed in OA MSCs compared with normal MSCs, using quantitative RT-PCR, whereas the expression of col1A2 mRNA chains was similar between OA and normal MSCs. This increase in col1A1 expression in OA MSCs without significant changes in col1A2 expression led to a significant increase in the ratio of col1A1 to col1A2 in OA MSCs compared with normal MSCs (**Figure 2F**). These results were supported by the data from western blot using col1A1 and col1A2 antibodies (**Figure 2G**).

IL-6 over-production in OA subchondral bone MSCs

Having observed the defective mineralization and abnormal type I collagen production in OA subchondral bone MSCs, we aimed to elucidate the underlying molecular mechanisms. Total

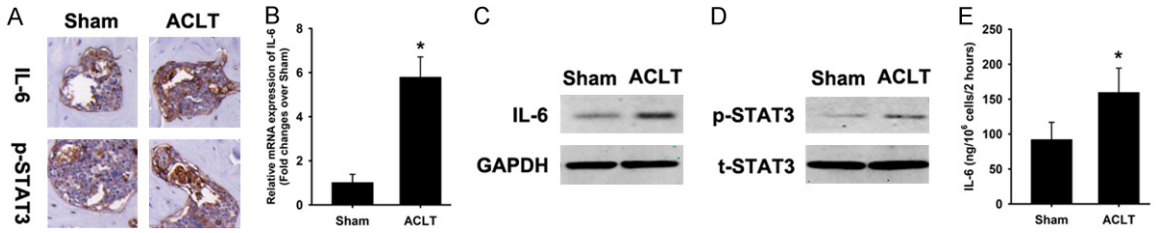

Figure 3. IL-6 over-production in OA subchondral bone MSCs. Immunostainings were employed to investigate the expression of IL-6 and p-STAT3 in the subchondral bone marrow of OA mice compared to sham controls (A). MSCs were harvested from subchondral bone of OA mice and sham controls, cultured *in vitro*. Quantitative RT-PCR was performed to investigate the mRNA expression level of IL-6 in OA MSCs compared with normal MSCs (B). GAPDH was used as an internal control. The results are expressed as the fold changes over Sham. Western blot was performed to investigate the expression levels of IL-6 (C) and p-STAT3 (D) in MSCs from OA and normal subchondral bone. GAPDH was used as an internal control. ELISA was employed to investigate the secretion of IL-6 from MSCs of OA and normal subchondral bone (E). Data are shown as the means ± SD. *: P<0.05, ACLT *vs.* Sham.

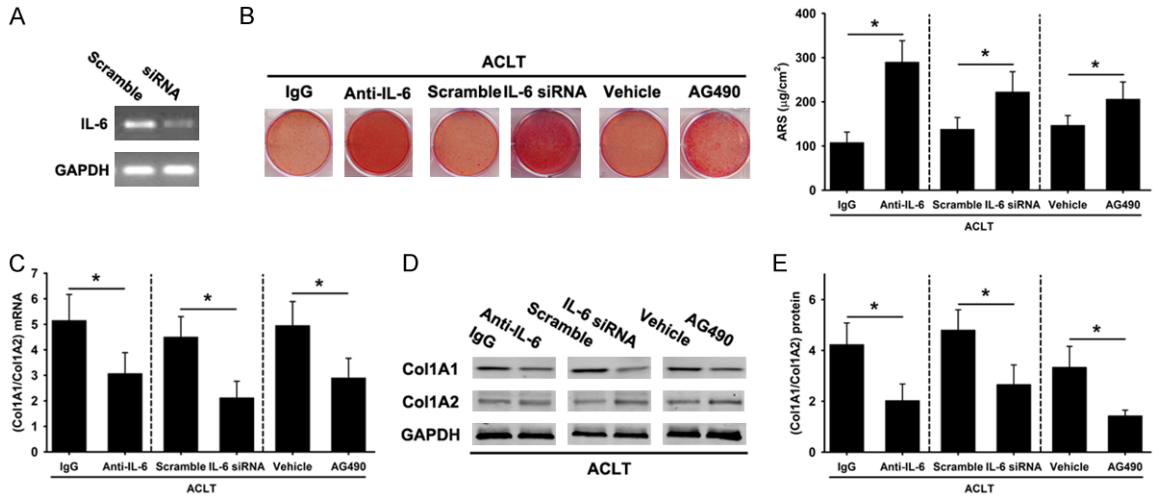

Figure 4. IL-6 contributes to the pathological phenotypes of OA subchondral bone MSCs. siRNA was employed to silence IL-6 expression in MSCs from OA subchondral bone (A). Following the treatment of IL-6 neutralization antibody, IL-6 siRNA or STAT3 inhibitor AG490, MSCs were induced to undergo osteogenic differentiation. Alizarin red staining was employed to evaluate the mineralization ability of these MSCs (B). Quantitative RT-PCR was performed to investigate the mRNA expression levels of col1A1 and col1A2 in OA MSCs treated with IL-6 neutralization antibody, IL-6 siRNA or STAT3 inhibitor AG490 and the ratio of col1A1 to col1A2 mRNA was calculated (C). GAPDH was used as an internal control. Western blot using col1A1 and col1A2 antibodies was performed to confirm the results from qRT-PCR (D). GAPDH was used as an internal control. Protein bands density was measured using image software (E). The relative protein expression level was normalized to GAPDH. Data are shown as the means ± SD. *: P<0.05.

protein was harvested from normal and OA MSCs. The protein expression levels of thirty-six bone metabolism markers were assessed using an antibody array. IL-6 was significantly upregulated in OA MSCs compared with normal control (Data not shown). Immunostaining revealed significant up-regulation of IL-6 in MSCs in tibia subchondral bone of OA mice compared with sham controls (**Figure 3A**). Immunostaining for phosphorylated STAT3 which is activated by IL-6 showed the same pattern as IL-6 (**Figure 3A**). qRT-PCR revealed a 5-fold increase in IL-6 mRNA expression in OA subchondral bone MSCs compared with normal MSCs (**Figure 3B**). Through western blot, significant protein up-regulation of IL-6 (**Figure 3C**) and phosphorylated STAT3 (**Figure 3D**) was observed in OA subchondral bone MSCs compared with normal MSCs. Supernatant of OA and normal MSCs was collected and ELISA was performed to measure the IL-6 secretion of these cells. The enhancement of IL-6 secretion was observed in OA subchondral bone MSCs compared with normal MSCs (**Figure 3E**). These data suggested IL-6 signaling was over-activated in OA subchondral bone MSCs.

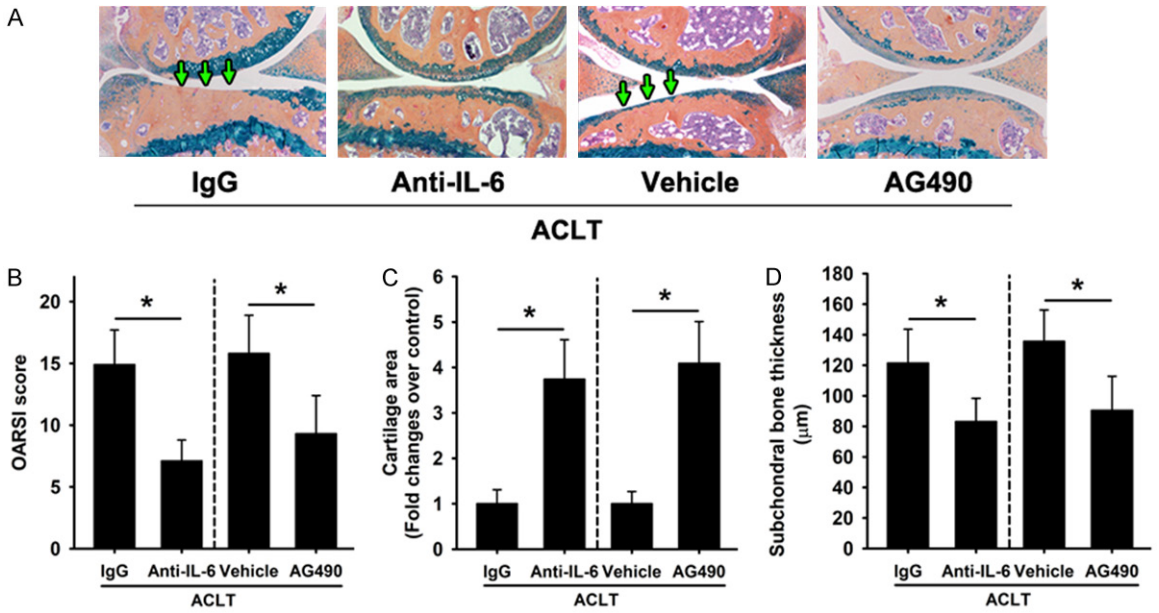

Figure 5. The alleviation of cartilage degradation and subchondral bone sclerosis in ACLT OA mouse in response to IL-6 signaling blockade. Anterior cruciate ligament transaction (ACLT) was performed in 8-week-old male C57BL/6 mice to induce OA. In a first assay, mice received intraperitoneal injections weekly of an IL-6 antibody or an IgG isotype control for 8 weeks from the day after the ACLT. In a second assay, the mice were treated daily with an intraperitoneal injection of AG490 or DMSO vehicle control for 8 weeks from the day after the ACLT. 8 weeks after surgery, histological changes in knee joints were analyzed between OA mice and sham controls by AB/H&OG staining (A). Green arrows indicated cartilage destructions. The summed OARSI scores of articular cartilage histologic structure were compared in OA mice or sham controls (B). The cartilage area of tibia was quantified through Bioquant software in OA mice and sham controls (C). The subchondral bone thickness of tibia was quantified in OA mice and sham controls (D). Data are shown as the means ± SD. *: $P < 0.05$.

IL-6 contributes to the pathological phenotypes of OA subchondral bone MSCs

We then asked whether IL-6 signaling over-activation contributed to the defective mineralization and abnormal type I collagen production in OA subchondral MSCs. To answer this question, we made attempts to block IL-6 signaling of OA MSCs through IL-6 neutralization antibody, IL-6 siRNA (**Figure 4A**) and STAT3 inhibitor AG490. Alizarin red staining revealed a significant enhancement of mineralization in OA subchondral bone MSCs in response to IL-6 signaling blockade (**Figure 4B**). These results were supported by the Alizarin red quantification (**Figure 4B**), suggesting that defective mineralization of OA MSCs was improved through IL-6 signaling blockade.

qRT-PCR revealed that the ratio of col1A1 to col1A2 mRNA in OA MSCs was reduced in response to IL-6 neutralization antibody, IL-6 siRNA and AG490 (**Figure 4C**). As shown in **Figure 4D**, the down-regulation of col1A1 protein was observed in OA MSCs in response to IL-6 neutralization antibody, IL-6 siRNA and AG490, using western blot, whereas the expression of col1A2 protein remained unchanged. This decrease in col1A1 protein expression in OA MSCs without significant changes in col1A2 protein expression in response to IL-6 signaling blockade led to a significant decrease in the ratio of col1A1 to col1A2 in OA MSCs (**Figure 4E**). These data suggested that the abnormal type I production in OA MSCs was corrected at least in part, if not all, through IL-6 signaling blockade.

The alleviation of cartilage degradation and subchondral bone sclerosis in ACLT OA mouse in response to IL-6 signaling blockade

To validate the role of IL-6 in the subchondral bone at the progression of osteoarthritis, we systemically injected IL-6 antibody or AG490, which was responsible for the blockade of IL-6 signaling, into OA mouse. The knee joints were harvested 8 weeks after surgery. AB/H&OG staining revealed a significant improvement of ACLT-induced cartilage degenerations and proteoglycans loss of knee joints in response to

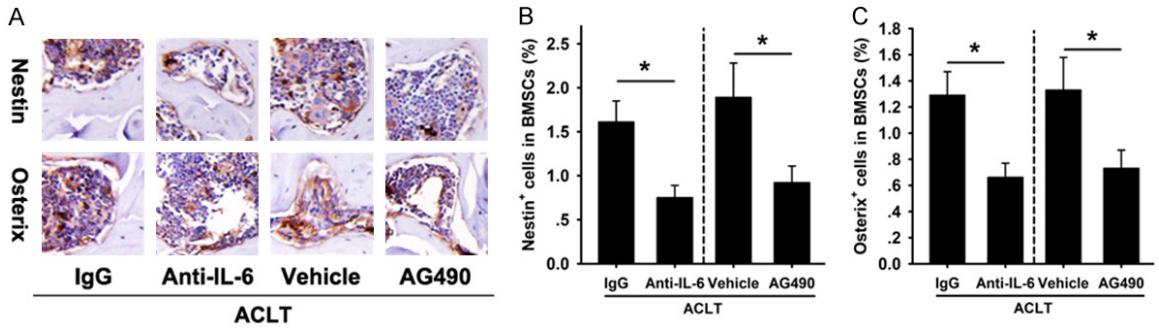

Figure 6. The decrease of subchondral bone MSCs number of OA mouse in response to IL-6 signaling blockade. Anterior cruciate ligament transaction (ACLT) was performed in 8-week-old male C57BL/6 mice to induce OA. In a first assay, mice received intraperitoneal injections weekly of an IL-6 antibody or an IgG isotype control for 8 weeks from the day after the ACLT. In a second assay, the mice were treated daily with an intraperitoneal injection of AG490 or DMSO vehicle control for 8 weeks from the day after the ACLT. 8 weeks after surgery, immunostainings for nestin and osterix were employed to analyze the number of MSCs in the subchondral bone marrow (A). Flow cytometry was performed to confirm the results from immunostainings (B and C). Data are shown as the means ± SD. *: $P<0.05$.

the use of IL-6 neutralization antibody or AG490 compared with IgG control or AG490 vehicle (**Figure 5A**). Correspondingly, the summed OARSI scores for morphological structure changes were significantly lower in the knee joints in response to the use of IL-6 neutralization antibody or AG490 (**Figure 5B**). A 3-fold increase in the tibia cartilage area was observed in the knee joints in response to the use of IL-6 neutralization antibody or AG490 (**Figure 5C**). The subchondral bone thickness of tibia was reduced significantly in response to the use of IL-6 neutralization antibody or AG490 compared with IgG control or AG490 vehicle (**Figure 5D**). These data suggested that cartilage degradation and subchondral bone sclerosis of OA mice was alleviated to some extent in response to IL-6 signaling blockade.

Immunostaining for nestin revealed a significantly lower number of nestin$^+$ cells in the subchondral bone marrow of OA mice in response to the use of IL-6 neutralization antibody or AG490 compared with IgG control or AG490 vehicle (**Figure 6A**). The number of osterix$^+$ osteoprogenitors also significantly decreased (**Figure 6A**). These results were confirmed in flow cytometry analysis. A significant decrease in the number of nestin$^+$ MSCs (**Figure 6B**) and osterix$^+$ osteoprogenitors (**Figure 6C**) from subchondral bone was observed in OA mice in response to IL-6 signaling blockade.

Discussion

Articular cartilage degradation is the primary pathological phenotype in OA, to which hypoxia-inducible factor-2α (HIF-2α) [27, 28] and complement component 5 (C5) [29] have been recently shown to contribute, in addition to ADAMTS5 [30] and MMP13 [31]. Articular cartilage homeostasis depends on its biochemical and biomechanical interaction with subchondral bone and other joint tissues such as synovium [32]. Subchondral bone provides the mechanical support for articular cartilage and undergoes modeling and remodeling in response to the mechanical environment changes [33]. For instance, ACL rupture increases the risk of knee OA [34]. It has been reported that about 20-35% of OA individuals are estimated to undergo an ACL tear [35]. Clinically, OA pathological phenotypes include cartilage degradation, tidemark disruption with angiogenesis, osteophyte formation and subchondral bone sclerosis [36]. Bone marrow lesion is always closely associated with pain and believed to predict the severity of cartilage damage in OA [37].

Both clinical and animal studies reported that the progression of OA is associated with the abnormal accumulation of MSCs in joint tissues and synovial fluids [38, 39]. We observed that IL-6 over-production from OA subchondral bone led to an increased number of nestin$^+$ and osterix$^+$ MSCs in the subchondral bone marrow in experimental OA model. During the normal remodeling process, osteoblasts and their progenitors are primarily recruited to the resorption site on the bone surface. However, the altered bone marrow microenvironment induced by abnormal mechanical loading may result in "*in situ*" commitment of osteoprogenitors in the bone marrow cavities. Less well mineralized

newly formed bone could be observed within bone marrow lesions [40]. These clustered bone marrow osteoprogenitors may lead to the *de novo* bone formation that is visualized as bone marrow lesions under MRI.

The alteration of the subchondral bone tissue microstructure in the progression of OA was recently described as osteogenesis imperfecta [41]. Therefore, subchondral bone sclerosis in OA may be attributable to abnormal collagen production *in vivo* [42]. Considering that type I collagen levels are enhanced in the trabecular bone of the femoral heads of OA patients, this should result in mineralization elevation [43]. However, the fact is that this tissue is observed to be hypo-mineralized [2, 5, 44]. Type I collagen is composed of a heterotrimer of α1 and α2 chains at an average ratio of 2.4:1 in normal subchondral bone. However, this ratio is elevated to 4:1-17:1 in *in vivo* OA bone tissue [42]. Associated with the reduction in crosslinks observed in OA bone tissue [2] and the overhydroxylation of lysine in collagen fibrils [42], this could explain a reduction in bone mineralization. However, whether the alterations of collagen production in OA subchondral bone could lead to abnormal cell metabolism or systemic regulation remains elusive.

Our results indicated that type I collagen production in OA MSCs is increased compared with normal MSCs and may be the cause of abnormal mineralization. This was resulted primarily from a direct effect on the col1A1 expression in OA MSCs. Associated with no significant change in col1A2 expression, this led to a higher ratio of α1 to α2 chain in OA MSCs than normal MSCs. Several previous reports have revealed a similar increase in expression of the α1 chain of type I collagen in *ex vivo* OA bone explants [45, 46]. We also observed a higher ratio of α1 to α2 chain in OA MSCs compared with normal MSCs, using Western blot. If *in vitro* conditions are similar *in vivo*, this would produce more type I collagen with an imbalance of α1 to α2 chains, which would impair proper mineralization. That is to say, although more abundant, this kind of collagen matrix is difficult to mineralize properly, which would result in a less mineralized subchondral bone. Futhermore, the decrease in mineralization observed *in vitro* under basal conditions indicated that a cellular defect is responsible for this abnormal mineral deposition so that osteogenic differentiation inducer such as BMP2 can not manage to correct this situation [47, 48].

IL-6 was previously shown to induce Mmp1, Mmp3 and Mmp13 and Adamts-4 and Adamts-5 mRNA expression in bovine chondrocytes [21]. IL-6 KO has been previously shown to reduce DMM-induced OA in mice [22]. In humans, a low production of IL-6 is associated with the absence of OA in the aged population [49]. Here, we showed that the systemic use of anti-IL-6 antibody or STAT3 inhibitor exerted protective effects in an experimental OA model, thus providing the relevance for IL-6 therapeutic targeting in OA. This finding supports ongoing clinical investigations of the efficacy of tocilizumab, a humanised anti-IL-6R monoclonal neutralising antibody, for severe subsets of OA patients (ClinicalTrials.gov NCT02477059).

ACLT-induced joint instability may lead to experimental OA through the mechanical stress on cartilage and subchondral bone. NF-κB is one of the most important transcription factors to modulate biomechanical signals in chondrocytes [50]. In OA, NF-κB also plays an important role [51]. IL-6 is not only a direct target gene of NF-κB in human chondrocytes [52], but also a key mediator of several chondrocyte procatabolic factors involved in OA. Our results suggested that the IL-6/Stat3 signaling might be another important regulator of catabolic and inflammatory effects of mechanical stress in OA-related cartilage damage and subchondral bone sclerosis. More importantly, IL-6 might crosstalk with other proinflammatory mediators such as IL-1 and TNFα in various joint tissues to contribute to the pathological phenotypes of OA.

Our findings are not unique. In a previous study, the authors reported that IL-6 induced chondrocyte catabolism mainly via Stat3 signaling, a pathway activated in cartilage from joint subjected to DMM. Systemic blockade of IL-6 or STAT-3 can alleviate DMM-induced OA in mice [53]. However, there are some important differences between these two studies. Firstly, unlike the previous study in which antibody against IL-6R was used to block IL-6 activity, monoclonal antibody against IL-6 was employed in the current study; secondly, AG490 was used to inhibit STAT3 activity in the current study and in contrast, Stattic was used in the previous study; finally, the previous study mainly focused

on the effect of IL-6 on articular cartilage and our study focused on the effect of IL-6 on subchondral bone. Coupled with the previous study, our study provides deeper insights into OA pathogenesis by demonstrating the pivotal role of the IL-6/Stat3 pathway in OA.

In conclusion, we showed that IL-6 was overproduced by OA subchondral bone MSCs and IL-6/Stat3 signaling was over-activated in OA subdhondral bone, which contributed to the pathological phenotypes of OA subchondral bone MSCs including MSCs number increase, mineralization disorder and abnormal type I collagen production. The systemic blockade of IL-6 signaling could alleviate the severity of cartilage degradation and subchondral bone sclerosis of experimental OA in mice. Our results open new therapeutic perspectives on the basis of the data that pharmacological blockade of the IL-6/Stat3 signaling could reduce OA severity. These findings need to be further confirmed with other blocking strategies (other pharmacological inhibitors, siRNA or gene knockout) in different OA models.

Acknowledgements

This study was supported by the Project of Key Research & Development Plan of Jiangsu Provincial Department of Science and Technology (Grant no. BE2016640), Health Innovation-Teams of Xuzhou (Grant no. XWCX201601).

Disclosure of conflict of interest

None.

Address correspondence to: Qiugen Wang, Department of Trauma Orthopaedic, Shanghai General Hospital of Nanjing Medical University, Shanghai 200080, China. Tel: +86-21-37798561; Fax: +86-21-37798561; E-mail: wangqiugen60@sina.com; Guangwang Liu, Department of Orthopedic Surgery, Xuzhou Central Hospital, Xuzhou Clinical School of Xuzhou Medical University, The Affiliated Xuzhou Hospital of Medical College of Southeast University, Xuzhou Clinical Medical College of Nanjing University of Chinese Medicine, Xuzhou 221009, Jiangsu, China. Tel: +86-18012018238; Fax: +86-18012018238; E-mail: guangwangliu@163.com

References

[1] Hilal G, Martel-Pelletier J, Pelletier JP, Ranger P and Lajeunesse D. Osteoblast-like cells from human subchondral osteoarthritic bone demonstrate an altered phenotype in vitro: possible role in subchondral bone sclerosis. Arthritis Rheum 1998; 41: 891-899.

[2] Mansell JP and Bailey AJ. Abnormal cancellous bone collagen metabolism in osteoarthritis. J Clin Invest 1998; 101: 1596-1603.

[3] Westacott CI, Webb GR, Warnock MG, Sims JV and Elson CJ. Alteration of cartilage metabolism by cells from osteoarthritic bone. Arthritis Rheum 1997; 40: 1282-1291.

[4] Radin EL and Rose RM. Role of subchondral bone in the initiation and progression of cartilage damage. Clin Orthop Relat Res 1986; 34-40.

[5] Li B and Aspden RM. Mechanical and material properties of the subchondral bone plate from the femoral head of patients with osteoarthritis or osteoporosis. Ann Rheum Dis 1997; 56: 247-254.

[6] Nieoullon A, Cheramy A and Glowinski J. Interdependence of the nigrostriatal dopaminergic systems on the two sides of the brain in the cat. Science 1977; 198: 416-418.

[7] Ding M, Danielsen CC and Hvid I. Bone density does not reflect mechanical properties in early-stage arthrosis. Acta Orthop Scand 2001; 72: 181-185.

[8] Ding M, Odgaard A and Hvid I. Changes in the three-dimensional microstructure of human tibial cancellous bone in early osteoarthritis. J Bone Joint Surg Br 2003; 85: 906-912.

[9] Singh JA, Saag KG, Bridges SL Jr, Akl EA, Bannuru RR, Sullivan MC, Vaysbrot E, McNaughton C, Osani M, Shmerling RH, Curtis JR, Furst DE, Parks D, Kavanaugh A, O'Dell J, King C, Leong A, Matteson EL, Schousboe JT, Drevlow B, Ginsberg S, Grober J, St Clair EW, Tindall E, Miller AS, McAlindon T. 2015 American College of Rheumatology Guideline for the treatment of rheumatoid arthritis. Arthritis Rheumatol 2016; 68: 1-26.

[10] Tanaka T, Narazaki M and Kishimoto T. Therapeutic targeting of the interleukin-6 receptor. Annu Rev Pharmacol Toxicol 2012; 52: 199-219.

[11] Mihara M, Hashizume M, Yoshida H, Suzuki M and Shiina M. IL-6/IL-6 receptor system and its role in physiological and pathological conditions. Clin Sci (Lond) 2012; 122: 143-159.

[12] Garbers C, Hermanns HM, Schaper F, Muller-Newen G, Grotzinger J, Rose-John S and Scheller J. Plasticity and cross-talk of interleukin 6-type cytokines. Cytokine Growth Factor Rev 2012; 23: 85-97.

[13] Dandona P, Aljada A and Bandyopadhyay A. Inflammation: the link between insulin resistance, obesity and diabetes. Trends Immunol 2004; 25: 4-7.

[14] Livshits G, Zhai G, Hart DJ, Kato BS, Wang H, Williams FM and Spector TD. Interleukin-6 is a significant predictor of radiographic knee osteoarthritis: the Chingford study. Arthritis Rheum 2009; 60: 2037-2045.
[15] Levinger I, Levinger P, Trenerry MK, Feller JA, Bartlett JR, Bergman N, McKenna MJ and Cameron-Smith D. Increased inflammatory cytokine expression in the vastus lateralis of patients with knee osteoarthritis. Arthritis Rheum 2011; 63: 1343-1348.
[16] Tsuchida AI, Beekhuizen M, Rutgers M, van Osch GJ, Bekkers JE, Bot AG, Geurts B, Dhert WJ, Saris DB and Creemers LB. Interleukin-6 is elevated in synovial fluid of patients with focal cartilage defects and stimulates cartilage matrix production in an in vitro regeneration model. Arthritis Res Ther 2012; 14: R262.
[17] Larsson S, Englund M, Struglics A and Lohmander LS. Interleukin-6 and tumor necrosis factor alpha in synovial fluid are associated with progression of radiographic knee osteoarthritis in subjects with previous meniscectomy. Osteoarthritis Cartilage 2015; 23: 1906-1914.
[18] Sanchez C, Gabay O, Salvat C, Henrotin YE and Berenbaum F. Mechanical loading highly increases IL-6 production and decreases OPG expression by osteoblasts. Osteoarthritis Cartilage 2009; 17: 473-481.
[19] Sellam J and Berenbaum F. The role of synovitis in pathophysiology and clinical symptoms of osteoarthritis. Nat Rev Rheumatol 2010; 6: 625-635.
[20] Eymard F, Pigenet A, Citadelle D, Flouzat-Lachaniette CH, Poignard A, Benelli C, Berenbaum F, Chevalier X and Houard X. Induction of an inflammatory and prodegradative phenotype in autologous fibroblast-like synoviocytes by the infrapatellar fat pad from patients with knee osteoarthritis. Arthritis Rheumatol 2014; 66: 2165-2174.
[21] Legendre F, Bogdanowicz P, Boumediene K and Pujol JP. Role of interleukin 6 (IL-6)/IL-6R-induced signal tranducers and activators of transcription and mitogen-activated protein kinase/extracellular. J Rheumatol 2005; 32: 1307-1316.
[22] Ryu JH, Yang S, Shin Y, Rhee J, Chun CH and Chun JS. Interleukin-6 plays an essential role in hypoxia-inducible factor 2alpha-induced experimental osteoarthritic cartilage destruction in mice. Arthritis Rheum 2011; 63: 2732-2743.
[23] Zhen G, Wen C, Jia X, Li Y, Crane JL, Mears SC, Askin FB, Frassica FJ, Chang W, Yao J, Carrino JA, Cosgarea A, Artemov D, Chen Q, Zhao Z, Zhou X, Riley L, Sponseller P, Wan M, Lu WW and Cao X. Inhibition of TGF-beta signaling in mesenchymal stem cells of subchondral bone attenuates osteoarthritis. Nat Med 2013; 19: 704-712.
[24] Glasson SS, Chambers MG, Van Den Berg WB and Little CB. The OARSI histopathology initiative-recommendations for histological assessments of osteoarthritis in the mouse. Osteoarthritis Cartilage 2010; 18 Suppl 3: S17-23.
[25] Weng T, Yi L, Huang J, Luo F, Wen X, Du X, Chen Q, Deng C, Chen D and Chen L. Genetic inhibition of fibroblast growth factor receptor 1 in knee cartilage attenuates the degeneration of articular cartilage in adult mice. Arthritis Rheum 2012; 64: 3982-3992.
[26] Couchourel D, Aubry I, Delalandre A, Lavigne M, Martel-Pelletier J, Pelletier JP and Lajeunesse D. Altered mineralization of human osteoarthritic osteoblasts is attributable to abnormal type I collagen production. Arthritis Rheum 2009; 60: 1438-1450.
[27] Saito T, Fukai A, Mabuchi A, Ikeda T, Yano F, Ohba S, Nishida N, Akune T, Yoshimura N, Nakagawa T, Nakamura K, Tokunaga K, Chung UI and Kawaguchi H. Transcriptional regulation of endochondral ossification by HIF-2alpha during skeletal growth and osteoarthritis development. Nat Med 2010; 16: 678-686.
[28] Yang S, Kim J, Ryu JH, Oh H, Chun CH, Kim BJ, Min BH and Chun JS. Hypoxia-inducible factor-2alpha is a catabolic regulator of osteoarthritic cartilage destruction. Nat Med 2010; 16: 687-693.
[29] Wang Q, Rozelle AL, Lepus CM, Scanzello CR, Song JJ, Larsen DM, Crish JF, Bebek G, Ritter SY, Lindstrom TM, Hwang I, Wong HH, Punzi L, Encarnacion A, Shamloo M, Goodman SB, Wyss-Coray T, Goldring SR, Banda NK, Thurman JM, Gobezie R, Crow MK, Holers VM, Lee DM and Robinson WH. Identification of a central role for complement in osteoarthritis. Nat Med 2011; 17: 1674-1679.
[30] Glasson SS, Askew R, Sheppard B, Carito B, Blanchet T, Ma HL, Flannery CR, Peluso D, Kanki K, Yang Z, Majumdar MK and Morris EA. Deletion of active ADAMTS5 prevents cartilage degradation in a murine model of osteoarthritis. Nature 2005; 434: 644-648.
[31] Neuhold LA, Killar L, Zhao W, Sung ML, Warner L, Kulik J, Turner J, Wu W, Billinghurst C, Meijers T, Poole AR, Babij P and DeGennaro LJ. Postnatal expression in hyaline cartilage of constitutively active human collagenase-3 (MMP-13) induces osteoarthritis in mice. J Clin Invest 2001; 107: 35-44.
[32] Lories RJ and Luyten FP. The bone-cartilage unit in osteoarthritis. Nat Rev Rheumatol 2011; 7: 43-49.
[33] Madry H, van Dijk CN and Mueller-Gerbl M. The basic science of the subchondral bone. Knee Surg Sports Traumatol Arthrosc 2010; 18: 419-433.

[34] Stein V, Li L, Lo G, Guermazi A, Zhang Y, Kent Kwoh C, Eaton CB and Hunter DJ. Pattern of joint damage in persons with knee osteoarthritis and concomitant ACL tears. Rheumatol Int 2012; 32: 1197-1208.
[35] Amin S, Guermazi A, Lavalley MP, Niu J, Clancy M, Hunter DJ, Grigoryan M and Felson DT. Complete anterior cruciate ligament tear and the risk for cartilage loss and progression of symptoms in men and women with knee osteoarthritis. Osteoarthritis Cartilage 2008; 16: 897-902.
[36] Suri S and Walsh DA. Osteochondral alterations in osteoarthritis. Bone 2012; 51: 204-211.
[37] Hunter DJ, Zhang Y, Niu J, Goggins J, Amin S, LaValley MP, Guermazi A, Genant H, Gale D and Felson DT. Increase in bone marrow lesions associated with cartilage loss: a longitudinal magnetic resonance imaging study of knee osteoarthritis. Arthritis Rheum 2006; 54: 1529-1535.
[38] Koyama N, Okubo Y, Nakao K, Osawa K, Fujimura K and Bessho K. Pluripotency of mesenchymal cells derived from synovial fluid in patients with temporomandibular joint disorder. Life Sci 2011; 89: 741-747.
[39] Sekiya I, Ojima M, Suzuki S, Yamaga M, Horie M, Koga H, Tsuji K, Miyaguchi K, Ogishima S, Tanaka H and Muneta T. Human mesenchymal stem cells in synovial fluid increase in the knee with degenerated cartilage and osteoarthritis. J Orthop Res 2012; 30: 943-949.
[40] Hunter DJ, Gerstenfeld L, Bishop G, Davis AD, Mason ZD, Einhorn TA, Maciewicz RA, Newham P, Foster M, Jackson S and Morgan EF. Bone marrow lesions from osteoarthritis knees are characterized by sclerotic bone that is less well mineralized. Arthritis Res Ther 2009; 11: R11.
[41] Blair-Levy JM, Watts CE, Fiorentino NM, Dimitriadis EK, Marini JC and Lipsky PE. A type I collagen defect leads to rapidly progressive osteoarthritis in a mouse model. Arthritis Rheum 2008; 58: 1096-1106.
[42] Bailey AJ, Sims TJ and Knott L. Phenotypic expression of osteoblast collagen in osteoarthritic bone: production of type I homotrimer. Int J Biochem Cell Biol 2002; 34: 176-182.
[43] Mansell JP, Tarlton JF and Bailey AJ. Biochemical evidence for altered subchondral bone collagen metabolism in osteoarthritis of the hip. Br J Rheumatol 1997; 36: 16-19.
[44] Mkukuma LD, Imrie CT, Skakle JM, Hukins DW and Aspden RM. Thermal stability and structure of cancellous bone mineral from the femoral head of patients with osteoarthritis or osteoporosis. Ann Rheum Dis 2005; 64: 222-225.
[45] Hopwood B, Tsykin A, Findlay DM and Fazzalari NL. Microarray gene expression profiling of osteoarthritic bone suggests altered bone remodelling, WNT and transforming growth factor-beta/bone morphogenic protein signalling. Arthritis Res Ther 2007; 9: R100.
[46] Truong LH, Kuliwaba JS, Tsangari H and Fazzalari NL. Differential gene expression of bone anabolic factors and trabecular bone architectural changes in the proximal femoral shaft of primary hip osteoarthritis patients. Arthritis Res Ther 2006; 8: R188.
[47] Hay E, Hott M, Graulet AM, Lomri A and Marie PJ. Effects of bone morphogenetic protein-2 on human neonatal calvaria cell differentiation. J Cell Biochem 1999; 72: 81-93.
[48] Yamagiwa H, Endo N, Tokunaga K, Hayami T, Hatano H and Takahashi HE. In vivo bone-forming capacity of human bone marrow-derived stromal cells is stimulated by recombinant human bone morphogenetic protein-2. J Bone Miner Metab 2001; 19: 20-28.
[49] Goekoop RJ, Kloppenburg M, Kroon HM, Frolich M, Huizinga TW, Westendorp RG and Gussekloo J. Low innate production of interleukin-1beta and interleukin-6 is associated with the absence of osteoarthritis in old age. Osteoarthritis Cartilage 2010; 18: 942-947.
[50] Knobloch TJ, Madhavan S, Nam J, Agarwal S Jr and Agarwal S. Regulation of chondrocytic gene expression by biomechanical signals. Crit Rev Eukaryot Gene Expr 2008; 18: 139-150.
[51] Marcu KB, Otero M, Olivotto E, Borzi RM and Goldring MB. NF-kappaB signaling: multiple angles to target OA. Curr Drug Targets 2010; 11: 599-613.
[52] Wang P, Zhu F and Konstantopoulos K. Prostaglandin E2 induces interleukin-6 expression in human chondrocytes via cAMP/protein kinase A- and phosphatidylinositol 3-kinase-dependent NF-kappaB activation. Am J Physiol Cell Physiol 2010; 298: C1445-1456.
[53] Latourte A, Cherifi C, Maillet J, Ea HK, Bouaziz W, Funck-Brentano T, Cohen-Solal M, Hay E and Richette P. Systemic inhibition of IL-6/Stat3 signalling protects against experimental osteoarthritis. Ann Rheum Dis 2017; 76: 748-755.